Supporting Information

Trap States Engineering toward All-Inorganic $CsPbBr_3$ Perovskite Nanocrystals for Highly Efficient Light-Emitting Diodes

*Xudong Jin,[a] Yanqin Miao,[a] Jianhua Dong,[a] Jingkun Wang,[a] Qiqing Lu,[a] Min Zhao,[*ab] Bingshe Xu[*a] and Junjie Guo[*a]*

a. Key Laboratory of Interface Science and Engineering in Advanced Materials of Ministry of Education, Taiyuan University of Technology, Taiyuan, Shanxi 030024, China

E-mail: zhaomin01@tyut.edu.cn, xubs@tyut.edu.cn, guojunjie@tyut.edu.cn

b. Aluminum-Magnesium Based New Material R&D Co., Ltd., Subsidiary of Xing Xian County Economic and Technological Development Zone, Xing Xian County, Shanxi 033699, China

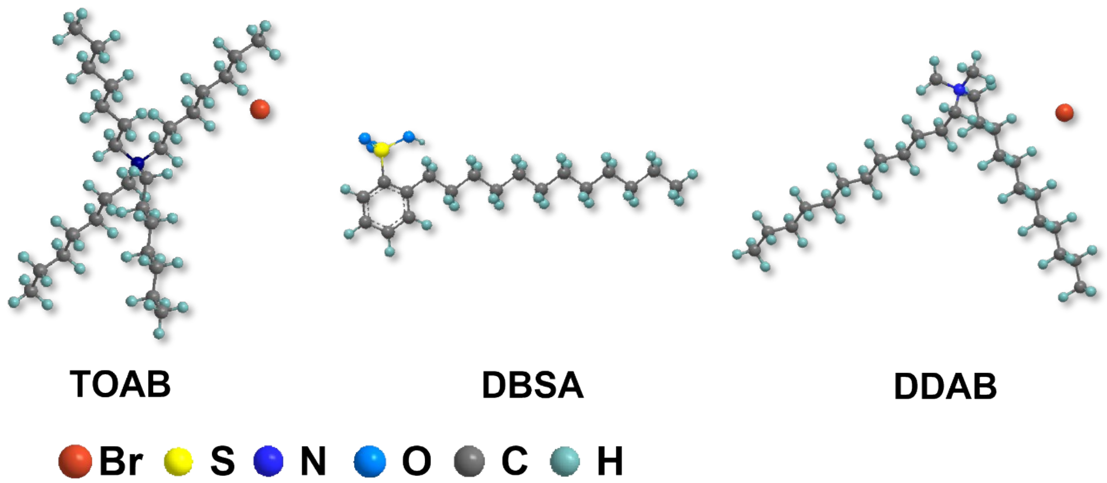

Fig. S1 Chemical structures of the surface ligands used in this work.

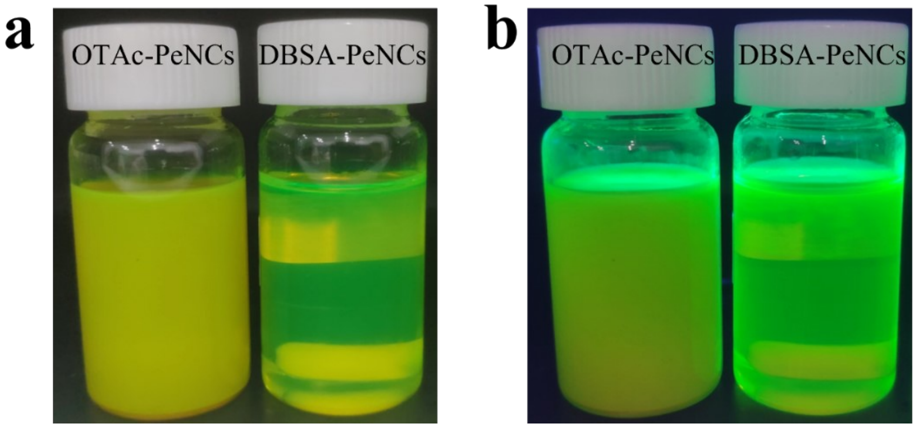

Fig. S2 The photographs of the crude solutions of the OTAc-PeNCs and DBSA-PeNCs under daylight (a) and UV-irradiation (b).

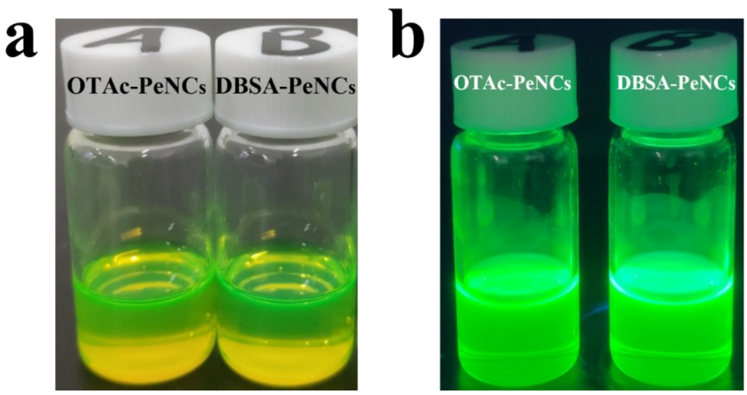

Fig. S3 The optical photographs of the OTAc-PeNCs (left) and DBSA-PeNCs (right) dissolved in toluene under day light (a) and under a 365 nm UV lamp (b).

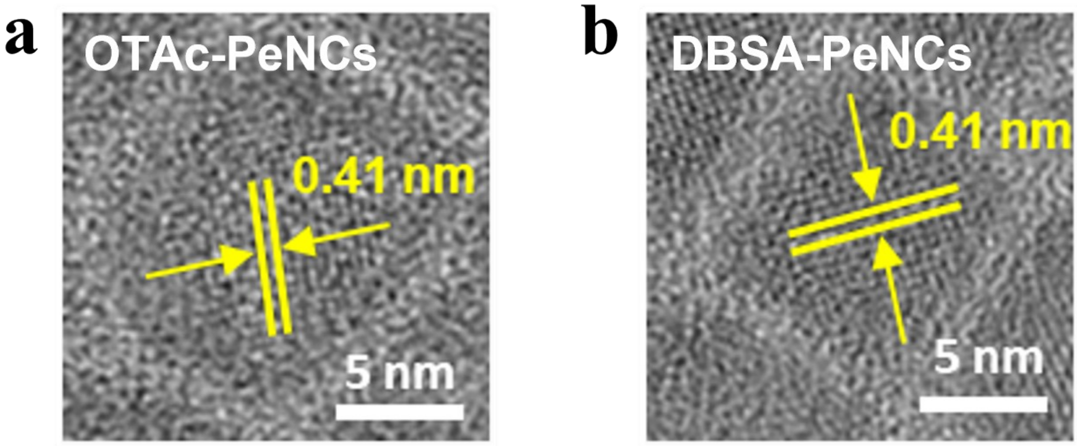

Fig. S4 The high-resolution TEM (HR-TEM) image for OTAc-PeNCs (a) and DBSA-PeNCs (b), respectively.

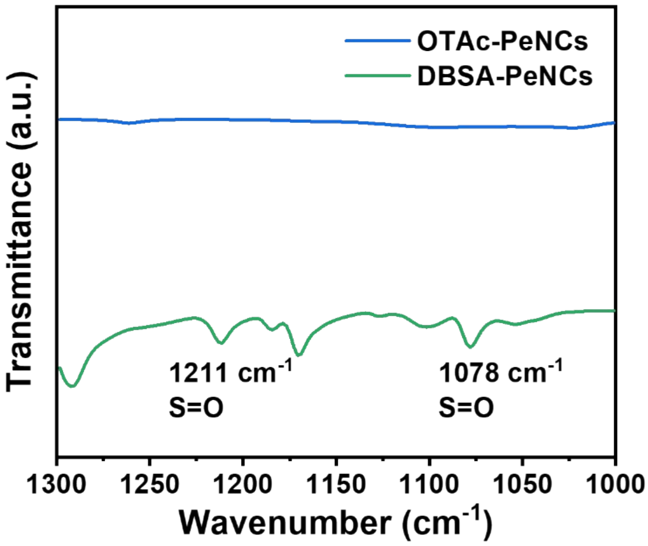

Fig. S5 FTIR spectra of OTAc-PeNCs and DBSA-PeNCs.

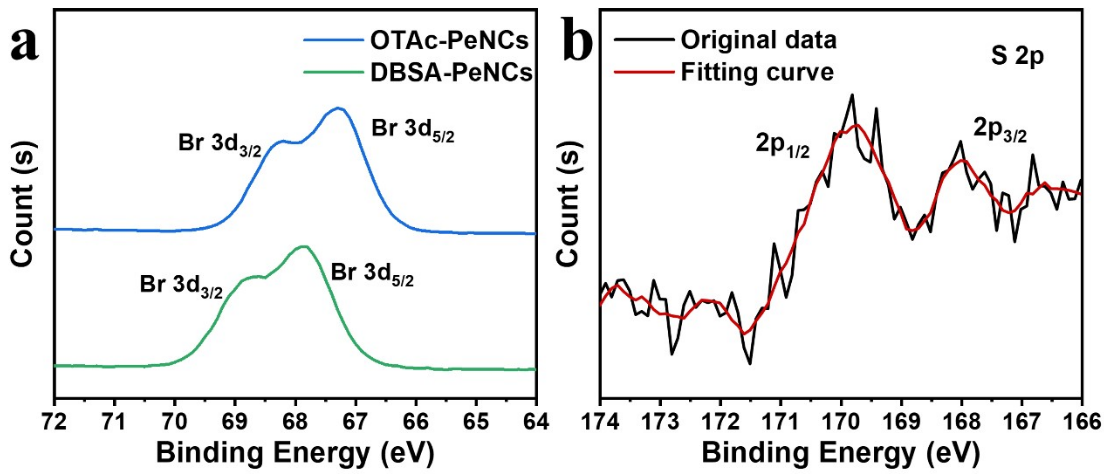

Fig. S6 (a) High-resolution XPS spectrum of the Br 3d signal in the OTAc-PeNCs film and DBSA-PeNCs film. (b) High-resolution XPS spectrum of the S 2p signal in the DBSA-PeNCs film.

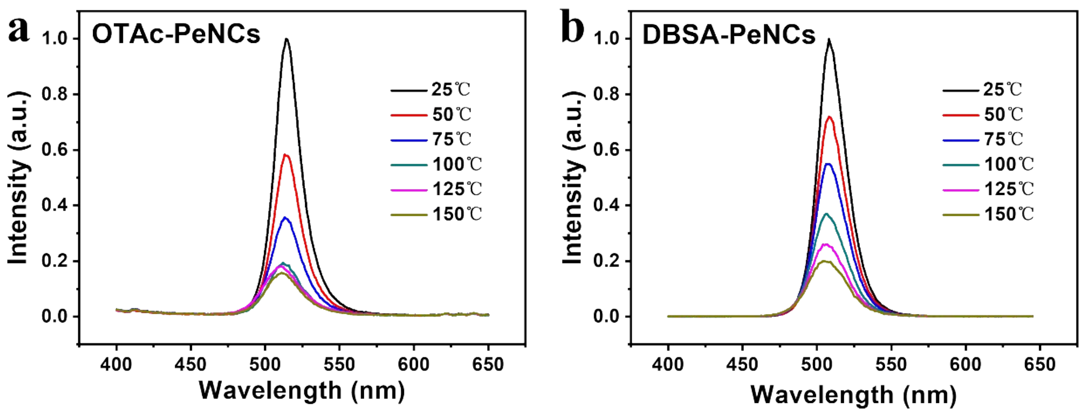

Fig. S7 Temperature-dependent PL behavior for OTAc-PeNCs (a) and DBSA- PeNCs (b).

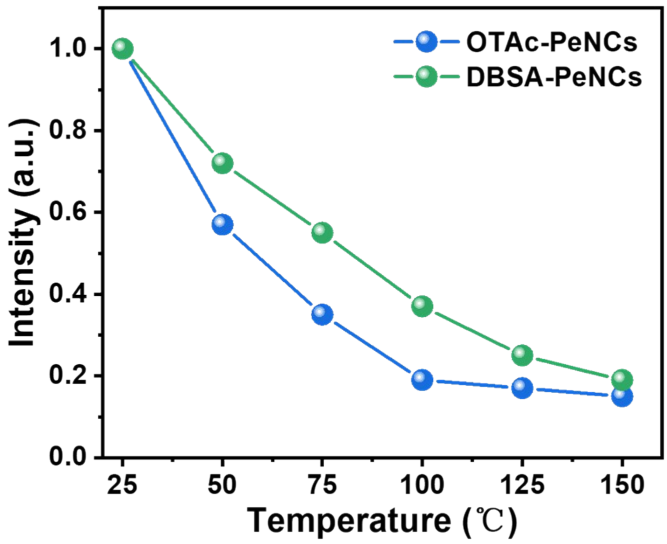

Fig. S8 High-temperature-dependent PL behavior of the peak emission intensity for OTAc-PeNCs and DBSA-PeNCs films.

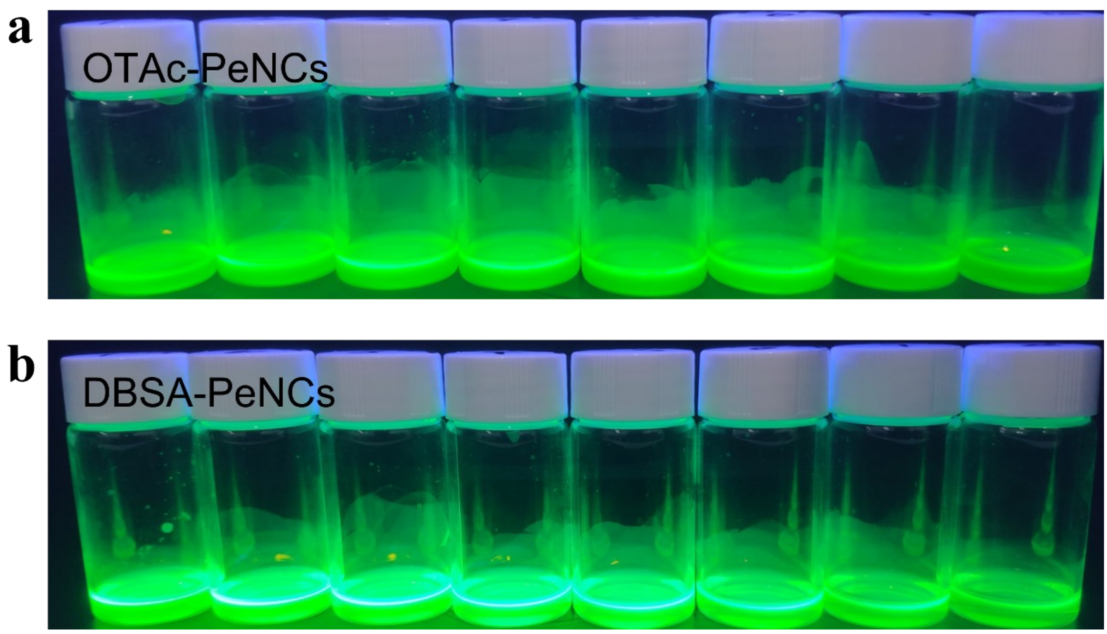

Fig. S9 Photograph of OTAc-PeNCs (a) and DBSA-PeNCs (b) after 1–8 cycles of purification under a 365 nm UV lamp, respectively.

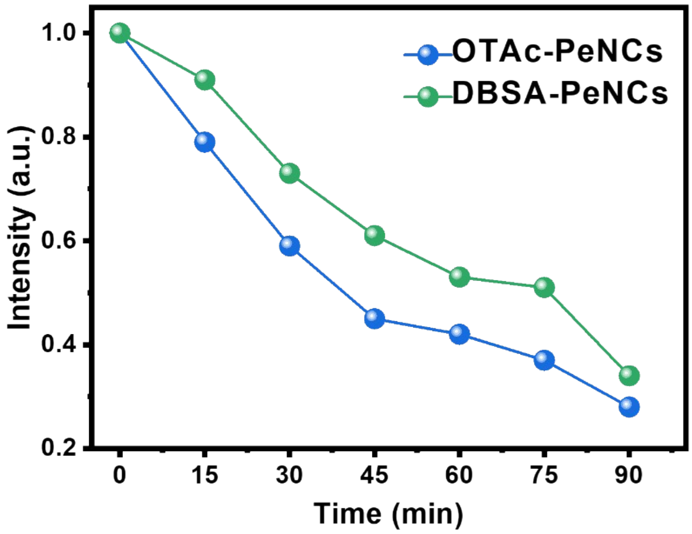

Fig. S10 The PL intensity of OTAc-PeNCs and DBSA-PeNCs under a sustained UV-light irradiation at room temperature.

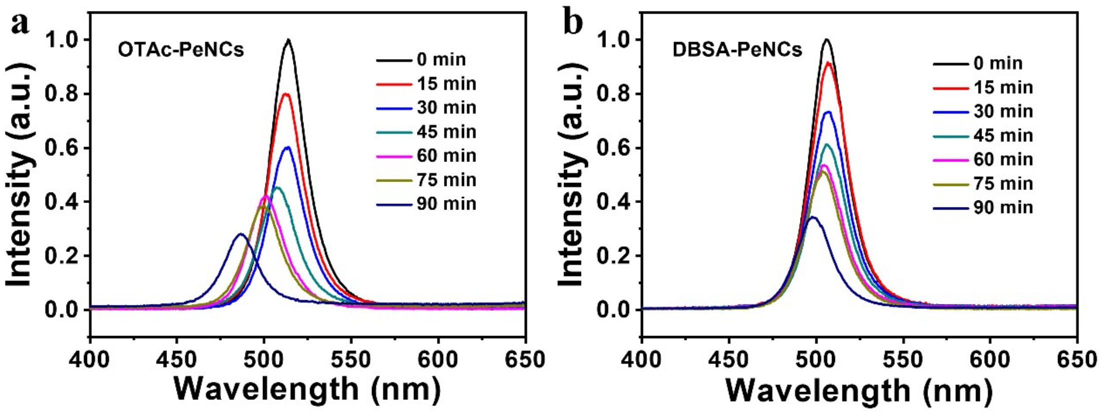

Fig. S11. Radiation-dependent PL behavior for OTAc-PeNCs (a) and DBSA-PeNCs (b).

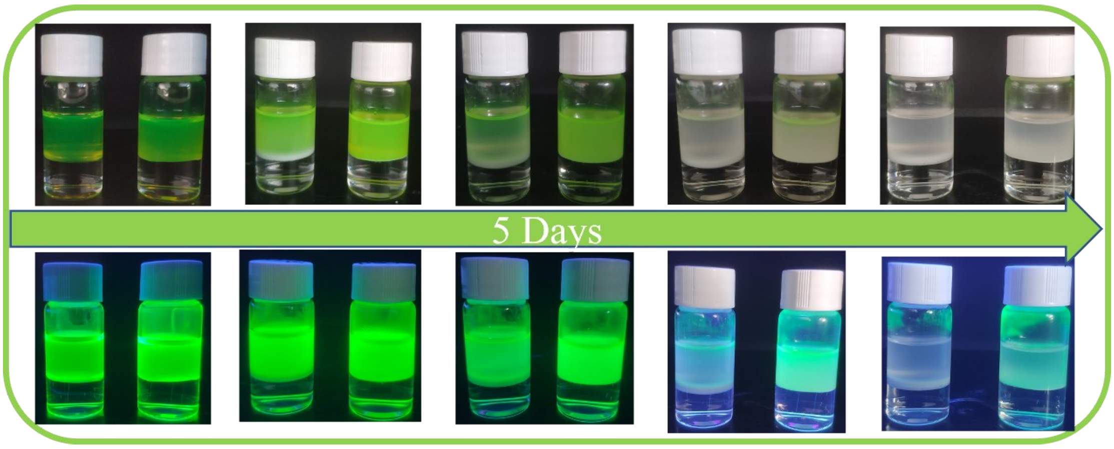

Fig. S12 Photographs showing the resistance against water treatment for OTAc-PeNCs (left) and DBSA-PeNCs (right) solution.

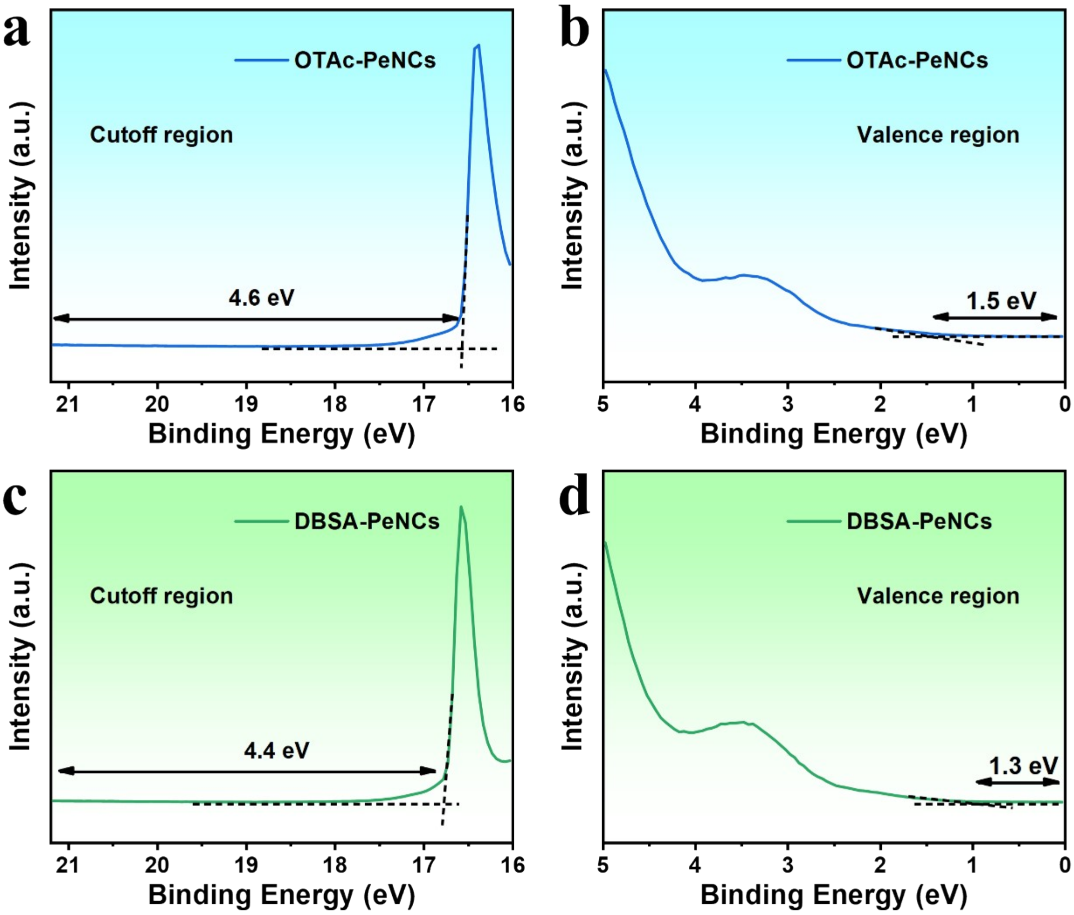

Fig. S13 Ultraviolet photoelectron spectra (UPS) at the high binding energy region (left) and at the low binding energy region (right) of OTAc-PeNCs (a, b) and DBSA-PeNCs films (c, d) on ITO substrates.

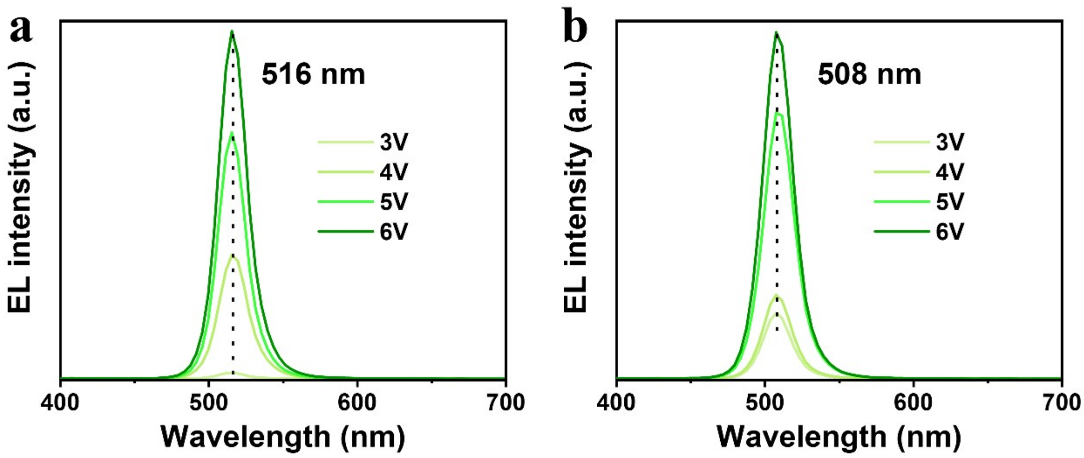

Fig.S14 EL spectra of OTAc-PeNCs (a) and DBSA-PeNCs (b) device under different applied voltages.

Table S1. Summary of EL performance of OTAc-PeNCs and DBSA- PeNCs PeLED device.

QLED	V_{on} (V)	L_{max} (cd/m^2)	CE (cd/A)	EQE (%)	PE (lm/W)	EL (nm)	CIE
OTAc	2.85	2339	9.1	2.75	9.59	516	(0.0981, 0.7592)
DBSA	2.8	4452	23.8	8.95	22.7	508	(0.0669, 0.6765)

Table S2. Summary of EL performance of reported PeLED devices based on $CsPbBr_3$ all-inorganic PeNCs.

Year	Categories	Synthesis method	EL (nm)	EQE (%)	CE (cd/A)	L_{max} (cd/m^2)	Refs.
2015	$CsPbBr_3$	HI	516	0.12	0.43	946	[1]
2016	$CsPbBr_3$	HI	516	0.06	0.19	1377	[2]
2016	$CsPbBr_3$	HI	510	0.325	-	934	[3]
2017	$CsPbBr_3$	HI	512	8.73	18.8	1660	[4]
2017	$CsPbBr_3$	HI	512	6.27	13.3	15185	[5]
2018	$CsPbBr_3$	HI	517	0.58	0.62	355	[6]
2018	$CsPbBr_3$	HI	518	4.626	8.736	10206	[7]
2019	$CsPbBr_3$	HI	-	7.74	-	1022	[8]
2019	$CsPbBr_3$	HI	513	9.7	31.7	2269	[9]
2020	$CsPbBr_3$	HI	513	9.1	-	24458	[10]
2020	$CsPbBr_3$	HI		22	-	-	[11]
2021	Na: $CsPbBr_3$	RT	525	8.97	34.5	20190	[12]
2021	$CsPbBr_3$	HI	-	13.4	-	1661	[13]
2022	Ca: $CsPbBr_3$	RT	-	10.5	-	63931	[14]
2023	$CsPbBr_3$	RT	508	8.95	23.8	4452	This work

References:

1. J. Song, J. Li, X. Li, L. Xu, Y. Dong and H. Zeng, *Adv. Mater*, 2015, **27**, 7162-7167.

2. X. Zhang, H. Lin, H. Huang, C. Reckmeier, Y. Zhang, W. C. Choy and A. L. Rogach, *Nano Lett*, 2016, **16**, 1415-1420.

3. E. Yassitepe, Z. Yang, O. Voznyy, Y. Kim, G. Walters, J. A. Castañeda, P. Kanjanaboos, M. Yuan, X. Gong, F. Fan, J. Pan, S. Hoogland, R. Comin, O. M. Bakr, L. A. Padilha, A. F. Nogueira and E. H. Sargent, *Adv. Funct. Mater*, 2016, **26**, 8757-8763.

4. T. Chiba, K. Hoshi, Y. J. Pu, Y. Takeda, Y. Hayashi, S. Ohisa, S. Kawata and J. Kido, *ACS Appl. Mater. Interfaces*, 2017, **9**, 18054-18060.

5. J. Li, L. Xu, T. Wang, J. Song, J. Chen, J. Xue, Y. Dong, B. Cai, Q. Shan, B. Han and H. Zeng, *Adv. Mater*, 2017, 29, 1603885-1603893.

6. W. Chen, X. Tang, P. Wangyang, Z. Yao, D. Zhou, F. Chen, S. Li, H. Lin, F. Zeng, D. Wu, K. Sun, M. Li, Y. Huang, W. Hu, Z. Zang and J. Du, *Adv. Opt. Mater*, 2018, **6**, 1800007-1800013.

7. Z. Shi, Y. Li, S. Li, X. Li, D. Wu, T. Xu, Y. Tian, Y. Chen, Y. Zhang, B. Zhang, C. Shan and G. Du, *Adv. Funct. Mater,* 2018, **28**, 1707031-1707041.

8. A. A. M. Brown, T. J. N. Hooper, S. A. Veldhuis, X. Y. Chin, A. Bruno, P. Vashishtha, J. N. Tey, L. Jiang, B. Damodaran, S. H. Pu, S. G. Mhaisalkar and N. Mathews, *Nanoscale*, 2019, **11**, 12370-12380.

9. J. H. Park, A. Y. Lee, J. C. Yu, Y. S. Nam, Y. Choi, J. Park and M. H. Song, *ACS*

Appl. Mater. Interfaces, 2019, **11**, 8428-8435.

10. J. S. Yao, J. C. Zhang, L. Wang, K. H. Wang, X. C. Ru, J. N. Yang, J. J. Wang, X. Chen, Y. H. Song, Y. C. Yin, Y. F. Lan, Q. Zhang and H. B. Yao, *J. Phys. Chem. Lett*, 2020, **11**, 9371-9378.

11. Y. Dong, Y. K. Wang, F. Yuan, A. Johnston, Y. Liu, D. Ma, M. J. Choi, B. Chen, M. Chekini, S. W. Baek, L. K. Sagar, J. Fan, Y. Hou, M. Wu, S. Lee, B. Sun, S. Hoogland, R. Quintero-Bermudez, H. Ebe, P. Todorovic, F. Dinic, P. Li, H. T. Kung, M. I. Saidaminov, E. Kumacheva, E. Spiecker, L. S. Liao, O. Voznyy, Z. H. Lu and E. H. Sargent, *Nat. Nanotechnol*, 2020, **15**, 668-674.

12. Y. Huang, P. Tang, W. Zhang, W. Yan, B. Liu, X. Tang, Z. Wang, Y. Peng and W. Chen, *J. Mater. Chem. C*, 2022, **10**, 3729-3737.

13. W. Zheng, Q. Wan, M. Liu, Q. Zhang, C. Zhang, R. Yan, X. Feng, L. Kong and L. Li, *J. Phys. Chem. C*, 2021, **125**, 3110-3118.

14. H. Shao, X. Wu, D. Zhou, W. Chen, L. Li, W. Xu, L. Xu, B. Dong, X. Bai and H. Song, *Small Methods*, 2022, **6**, 2200163-2200171.